

Study on the Propagation Law of Shock Wave Pressure in Tunnels with Different Materials

CHEN Jiahui, KONG Deren

(*Nanjing University of Science and Technology, Nanjing 210094*)

Abstract: The propagation of shock wave pressure in the tunnel is greatly affected by the tunnel structure, shape, material and other factors, and there are great differences in the propagation law of shock wave pressure in different kinds of tunnels. In order to study the propagation law of shock wave pressure in tunnels with different materials, taking the long straight tunnel with the square section as an example, the AUTODYN software is used to simulate the explosion of TNT in the concrete, steel and granite tunnel, and study on the variation law of shock wave pressure in tunnels with different materials. By using dimensional analysis and combined with the results of numerical simulation, a mathematical model of the propagation law of shock wave pressure in the tunnel is established, and the effectiveness of the mathematical model is verified by making the explosion test of the warhead in the reinforce concrete tunnel. The results show that the same mass of TNT explodes in the tunnel with different materials, and the shock wave overpressure peak at the same measuring point is approximate in the near field. However, there is a significant difference in the middle-far fields from the explosion center, the shock wave overpressure peak in the steel tunnel is 20.76% and 34.82% higher than that of the concrete and the granite tunnel respectively, and the shock wave overpressure peak in the concrete tunnel is 24.91% higher than that in the granite tunnel. Through the experimental verification, getting the result that the maximum relative deviation between the measured value and the calculated value of the shock wave overpressure peak is 11.85%. Therefore, it is proved that the mathematical model can be used to predict the shock wave overpressure peak in the tunnel with different materials, and it can provide some reference for the power evaluation of warhead explosion in the tunnel.

Keywords: Tunnel, Shock Wave Pressure, Numerical Simulation, Propagation Law

1 Introduction

The shock wave is the main kill element of warhead explosion in the tunnel, so it is of great significance to study the propagation law of shock wave pressure in the tunnel to evaluate the explosion power of the warhead accurately. Different from the explosion in free space, when the shock wave pressure propagates in the tunnel, due to the limitation of space, the shock wave pressure occurs multiple reflections and superposition after reaching the inner wall of the

tunnel, which makes the shock wave overpressure peak increase obviously, attenuate slowly and prolong the action time^[1-2]. The propagation law of shock wave pressure differs in different types of tunnels. Domestic and foreign scholars have carried out a lot of research on the propagation law of shock wave pressure in tunnels. Ma studied the propagation law of shock wave pressure in tunnels with different cross-section shapes by numerical simulation^[3]. Zhang obtained a model of shock wave pressure propagation in a square tunnel by making an explosion test in a square tunnel^[1]. Guo and

Zhong studied the propagation law of shock wave pressure in the tunnel when the explosive detonation at different positions^[4-5]. Song studied the influence of different both explosive heights and shapes of TNT on the propagation law of shock wave pressure in tunnels by numerical simulation^[6]. Li studied the difference on the propagation law of the shock wave pressure in the tunnel with different lining materials by making explosion test in the tunnel^[7]. Through the numerical simulation, Geng studied the difference of shock wave overpressure peak and other parameters between TNT and a specific type of thermo-baric explosive detonation in tunnel^[8]. Qu studied the propagation law of shock waves in different shapes of tunnels by numerical simulation^[9].

Most of the above studies on the propagation law of shock wave pressure in tunnel are based on the reinforced concrete tunnel. However, according to the geographical environment and different applications, tunnels can be built with various materials, such as concrete, steel, and granite, etc. Taking the long straight tunnel with square section as an example, through the nonlinear dynamic analysis software AUTODYN, the numerical simulation of TNT explosion in the concrete, steel and granite tunnel is carried out, then study on the propagation law of shock wave pressure in tunnel with different materials. Based on dimensional analysis and combined with the results of numerical simulation, a mathematical model of shock wave pressure propagation in the tunnel was

established, and the effectiveness of the model is verified by the explosion test of the warhead in the reinforce concrete tunnel.

2 Numerical Simulation

2.1 Model Establishment

Using the AUTODYN software to establish a tunnel model with an inner section size of 100mm×100mm and length of 3500mm. The thickness of the tunnel wall are all 30mm. The tunnel structure is modelled by the Lagrange element, and the air and TNT are modelled by the Euler element. The TNT is located at the centre of the section 500mm from the end of the tunnel. The mass of TNT is 20g, its shape is a cylinder with an aspect ratio of 1, and set as the center point to detonate. Using the ALE algorithm for simulation calculation. Considering the computer's computing power and ensuring the calculation accuracy, therefore, defining the air and tunnel model's grid size is 5mm, and the TNT model's grid size is 1mm. The part of air at both ends of the tunnel is set to the boundary as Flow-out, and the tunnel floor is set to fixed support. Starting from the distance from the explosion center 500mm, set up a Gaussian monitoring point at every interval of 100mm at the geometric centre of the plane where the side and bottom walls of the tunnel are located, where Gauge1~ Gauge26 are the side wall monitoring points, Gauge26~ Gauge52 are the bottom wall monitoring points. The tunnel finite element model is shown in Fig.1.

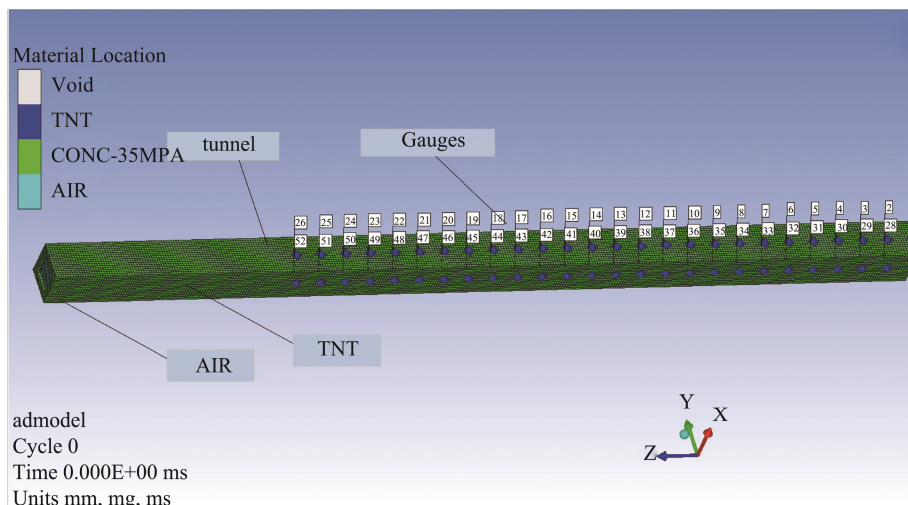


Fig.1 Finite Element Simulation Model

2.2 Material Model and Parameter Determination

2.2.1 Air Material Model

The air material model can be simplified to an inviscid ideal gas, and the expansion process of the shock wave pressure is assumed to be an adiabatic process, so the Linear-Polynomial equation of state is used to describe the air material^[10]. The specific parameters of the material model and equation of state are listed in Table 1.

2.2.2 Explosive Material Model

The explosive model was chosen as TNT, and the detonation product is described by the JWL equation of state^[11]. The specific parameters of the TNT model and equation of state are listed in Table 2.

2.2.3 Tunnel Material Model

(1) Concrete Material Model

The RHT material model was chosen according to the concrete multivacancy material properties, and its

equation of state is the P-alpha model^[12]. The main parameters of the concrete material and equation of state are listed in Table 3.

(2) Steel Material Model

Structural steel was chosen as the steel material, using the Johnson-Cook model and the Linear equation of state^[13]. The specific material parameters are listed in Table 4.

(3) Granite Material Model

The JH-2 material model was chosen to characterize the nonlinear deformation features of granite material under the high-pressure impact, and its equation of state can be described as^[14]:

$$P = k_1\mu + k_2\mu^2 + k_3\mu^3 \quad (1)$$

In the formula, k_1 is the bulk modulus, k_2, k_3 is the pressure constant, $\mu = \rho/\rho_0 - 1$ is the volume strain, and ρ_0 is the initial density. The parameters of the material model and equation of state are shown in Table 5.

Table 1 The Parameters of Air Material Model and State Equation

Initial Density (g/cm ⁻³)	Initial Pressure (Pa)	Initial Internal Energy (mJ/mm ³)	Adiabatic Exponent
1.293	1×10 ⁵	2.068×10 ⁵	1.4

Table 2 The Parameters of TNT Model and Equation of State

Density (g/mm ⁻³)	C-J Pressure (kPa)	Detonation Velocity (m·s ⁻¹)	A (kPa)
1.63	2.1×10 ⁷	6930	3.74×10 ⁸
B (kPa)	ω	R ₁	R ₂
3.75×10 ⁶	0.35	4.15	0.9

Table 3 The Parameters of Concrete Material Model and State Equation

Initial Density (g/cm ⁻³)	Compaction Pressure (kPa)	Compression Index	Shear Modulus (kPa)
2.75	6×10 ⁶	3.00	2.2×10 ⁷
Compressive Strength (kPa)	Tensile Strain Rate	Failure Surface Constant	A ₁ (kPa)
1.4×10 ⁵	0.0125	1.6	3.52×10 ⁷
A ₂ (kPa)	A ₃ (kPa)	B ₀	B ₁
3.96×10 ⁷	9.04×10 ⁷	1.22	1.22

Table 4 The Parameters of the Johnson-cook Model and State Equation of Structural Steel

Density (g/mm ⁻³)	A (kPa)	B (kPa)	n
7.85	7.92×10 ⁵	5.1×10 ⁵	0.26
C	m		
0.014	1.03		

2.3 The Results of Simulation and Analysis

The pressure curves of the monitoring points at the inner side and bottom of the tunnel at the distance from the explosion center 500mm, 900mm and 1300mm in tunnel with different materials are selected as shown in Fig.2. It can be seen from the figure that the shock wave overpressure peak at different pressure monitoring points at the same distance from the explosion centre are almost equal. Due to the constraint of the tunnel space, the shock wave pressure is repeatedly reflected and superimposed during the propagation process, so the shock wave pressure curve has multiple peaks and attenuates slowly. With the

increase of the blasting center distance, the shock wave overpressure peak decreases gradually, and the shock wave pressure at different monitoring points attenuate to a certain pressure value and no longer continue to attenuate. The pressure flow in the tunnel gradually tends to be stable and sustained for a long time.

Since the tunnel is a regular square cross-section tunnel, the shock wave overpressure peak and its time history curve at different monitoring points of the plane where the same explosion center is located are similar in near-middle-far fields from the explosion center. Therefore, the subsequent content only selects the shock wave pressure of the monitoring points on the side wall of the tunnel for analysis.

Table 5 The Parameters of the JH-2 Material Model and Equation of State

Density (g/mm^3)	Poisson Ratio	Elastic Modulus (kPa)	Shear Modulus (kPa)
2.657	0.29	8×10^9	3.001×10^7
k_1 (kPa)	k_2 (kPa)	k_3 (kPa)	D_1
6.334×10^7	4.48×10^8	-2.556×10^9	0.005
D_2	G_f (J/m^2)		
0.68	70		

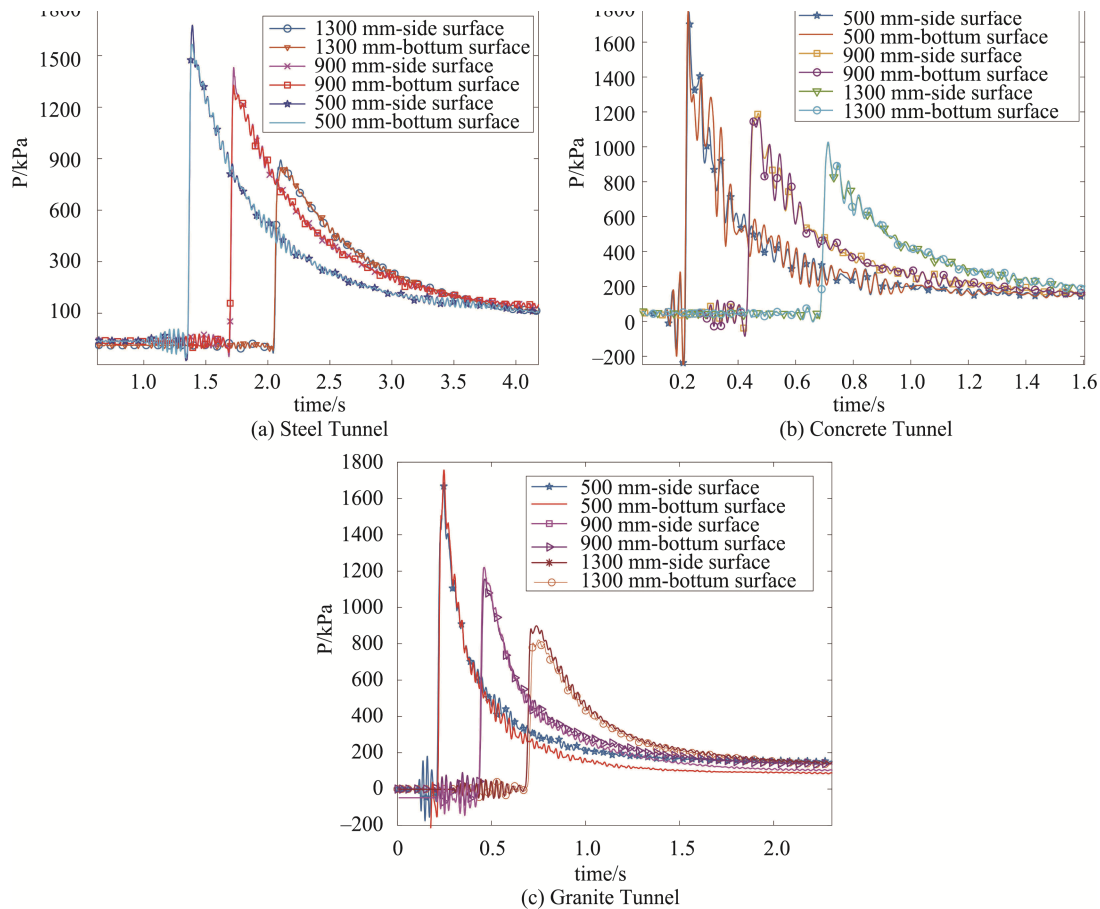


Fig.2 Shock Wave Pressure Curve

Selecting the pressure monitoring points at the distance from the explosion center 500mm, 1600mm and 2300mm in the tunnel with different materials of concrete, steel and granite and the shock wave pressure curve are shown in Fig.3. It can be seen from the figure when the same mass of TNT explodes in tunnels with different materials, the shock wave overpressure peak and its time history curve are almost equal in the near-field from the explosion center. With the increase of the blast center distance, the shock wave overpressure peak in the tunnel with different materials is different obviously. When the blast center distance is same, the shock wave overpressure peak is the highest in the steel tunnel, followed by the concrete tunnel, and the lowest in the granite tunnel.

Because the two ends of the tunnel are open when the TNT explodes in the tunnel, the pressure relief is

obvious at the position of the tunnel mouth (3000mm from the explosion center). In order to more accurately study the propagation law of shock wave pressure in the tunnel, the shock wave overpressure peak at this monitoring point is ignored. According to the numerical simulation results, the shock wave overpressure peak at different blast center distances in the tunnels with different materials are obtained as listed in Table 6.

The variation curve of the shock wave overpressure peak at different blast center distances from the explosion point in tunnel with different materials is shown in Fig.4. It can be seen that the same mass TNT explodes in tunnels with different materials, the shock wave overpressure peak in steel tunnel is higher than that in other tunnels at the same distance from the explosion point. It can be obtained by calculating that shock wave overpressure peak in the

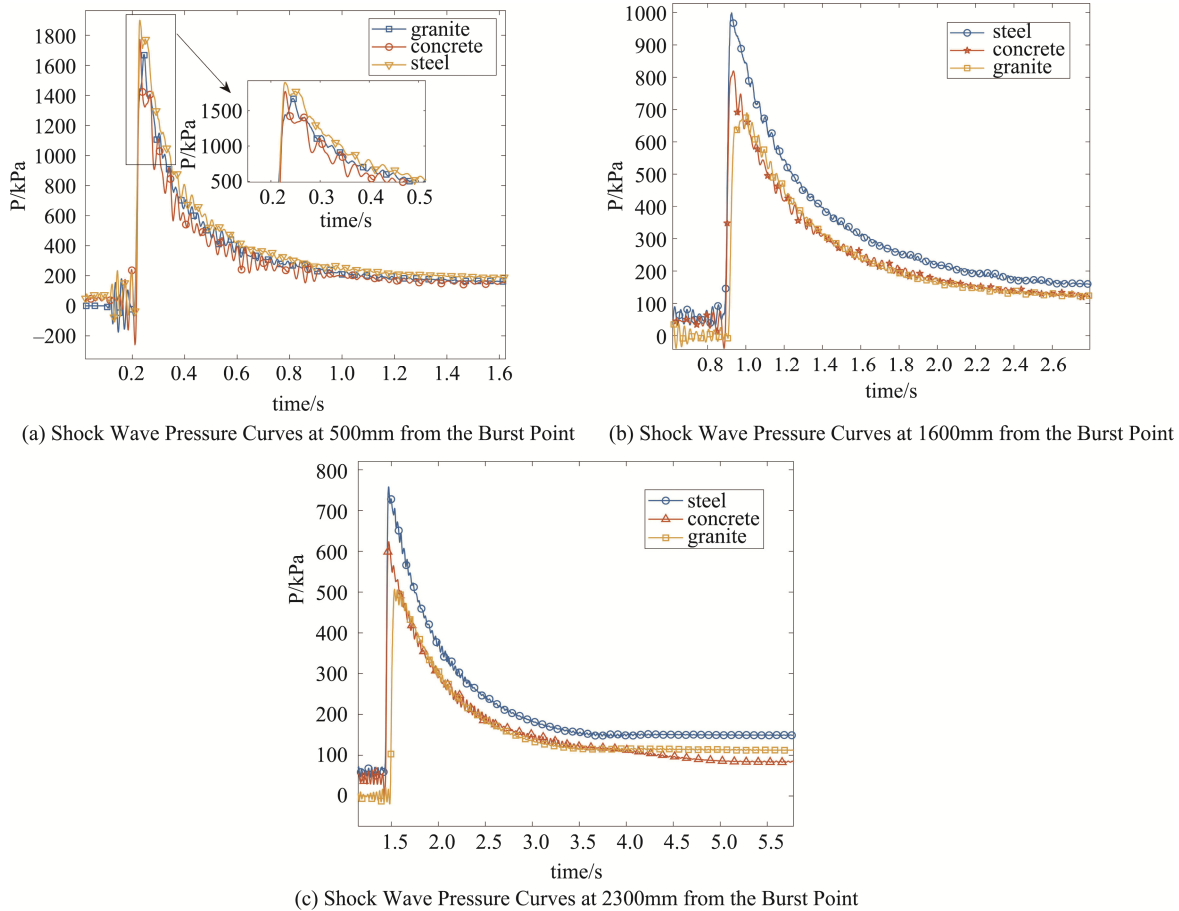


Fig.3 Shock Wave Pressure Curves in Near-mid-far Field

Table 6 Shock Wave Overpressure Peak at Different Blast Distances

Blast Center Distance (mm)	Pressure (kPa)		
	Concrete	Steel	Granite
500	1772.30	1899.50	1672.70
600	1632.20	1802.10	1540.30
700	1496.80	1755.70	1434.80
800	1295.70	1575.20	1255.50
900	1191.20	1503.30	1156.30
1000	1164.20	1366.50	1025.10
1100	1114.90	1309.30	946.56
1200	993.11	1215.60	896.89
1300	1018.50	1147.80	820.72
1400	896.48	1111.50	764.35
1500	922.44	1040.30	713.78
1600	819.56	999.38	689.85
1700	819.62	950.03	653.21
1800	786.40	907.03	619.08
1900	721.28	873.44	586.72
2000	711.99	848.74	557.93
2100	698.17	821.40	535.38
2200	658.89	792.81	518.90
2300	623.58	757.89	506.89
2400	603.06	721.79	488.56
2500	591.75	707.94	469.59
2600	576.71	687.19	452.02
2700	560.25	656.45	448.78
2800	544.60	646.10	431.04
2900	530.70	631.30	415.88

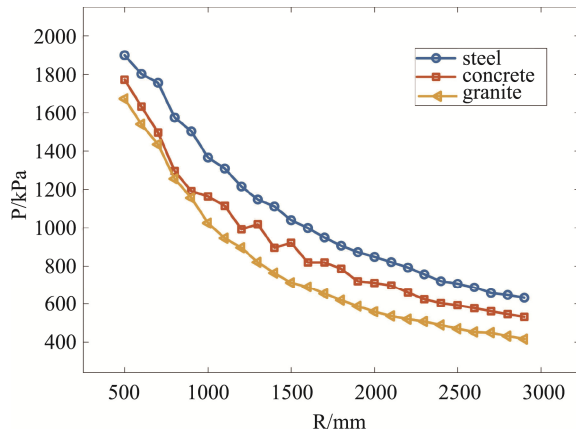


Fig.4 Variation Curve of Shock Wave Pressure Peak

steel tunnel is 20.76 % higher than that in the concrete tunnel and 34.82 % higher than that in the granite tunnel. In the near-field from the explosion center, the difference of the shock wave overpressure peak between in the concrete tunnel and in the granite tunnel is obvious. With the increase of blast center distance, the shock wave overpressure peak in the concrete tunnel is significantly higher than that in the granite tunnel, the maximum is 24.91 % higher than that in the granite tunnel.

The attenuation rate curve of the shock wave overpressure peak at every two adjacent monitoring points in tunnel with different materials is shown in Fig.5. It can be seen from the figure that the attenuation rate of shock wave overpressure peak changes with the trend of downward-increasing-downward, and the variable range of shock wave pressure attenuation rate is the largest in the concrete tunnel. The shock wave overpressure peak attenuation rate in the steel and granite tunnel is almost equal, and the two adjacent monitoring points' shock wave pressure peak attenuation rate is less than 15 %. In the near-field from the explosion center, the attenuation rate of shock wave overpressure peak in the steel tunnel is the lowest. The attenuation rate of the shock wave overpressure peak in the concrete tunnel is the highest in the range of 1300 to 1600 from the explosion point. With the increase of the blast center distance, the attenuation rate of shock wave overpressure peak in tunnels with different materials tends to be equal approximately, and all are less than 5%. The shock wave pressure attenuates slowly and sustains for a long time in the tunnel.

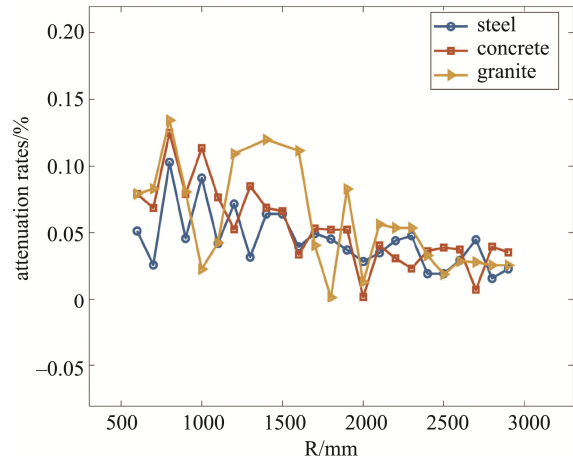


Fig.5 Attenuation Rate Curve of Shock Wave Pressure Peak

2.4 Study on the Propagation Law of Shock Wave Pressure in Tunnel

When both ends of the tunnel are open, the TNT explodes in the tunnel, and the factors that affect the shock wave pressure propagation in the tunnel mainly include the charge of TNT W , kg; the air density in the tunnel ρ_0 , kg/m³; the sound velocity C_0 , m/s; the material density of tunnel ρ , kg/m³; the strength of tunnel σ , MPa; the cross-section of tunnel S , m²; and the blasting center distance R , m. Because the TNT

explodes in the tunnel, the pressure measuring points are all in the interior of the tunnel, the blast center distance can indicate the length of the tunnel; so the shock wave overpressure peak in the tunnel can be expressed as :

$$P = \Psi(W, \rho_0, C_0, \rho, \sigma, R, S) \quad (2)$$

Taking the mass M, length L and time T as the basic dimensions, the dimensions of physical quantity involved above are shown in Table 7.

Table 7 Influence Parameters and Corresponding Dimensions of Shock Wave Pressure in Tunnel

Physical Quantity	Dimension	Physical Quantity	Dimension
W	M	σ	$ML^{-1}T^{-2}$
ρ_0	ML^{-3}	S	L^2
C_0	LT^{-1}	R	L
ρ	ML^{-3}	P	$ML^{-1}T^{-2}$

According to the Π theorem, the five dimensionless quantities are obtained:

$$\Pi_1 = \frac{\rho}{\rho_0}, \Pi_2 = \frac{\sigma}{\rho_0 \cdot C_0^2}, \Pi_3 = \frac{\rho^{2/3} \cdot S}{W^{2/3}}, \Pi_4 = \frac{\rho^{1/3} \cdot R}{W^{1/3}},$$

$$\Pi_5 = \frac{P}{\rho_0 \cdot C_0^2}.$$

Thus, the following formula can be obtained:

$$\frac{P}{\rho_0 \cdot C_0^2} = \Psi\left(\frac{\rho}{\rho_0}, \frac{\sigma}{\rho_0 \cdot C_0^2}, \frac{\rho^{2/3} \cdot S}{W^{2/3}}, \frac{\rho^{1/3} \cdot R}{W^{1/3}}\right) \quad (3)$$

The formula (3) can be further simplified to get:

$$P = \Psi\left(\frac{R \cdot S}{W} \cdot \rho \cdot \sigma\right) \quad (4)$$

According to the numerical simulation results in Table 6, and substituting the physical values involved in equation (8), the following formula is obtained by fitting:

$$P = 1317 \left(\frac{R \cdot S}{W} \cdot \rho \cdot \sigma\right)^{-0.6578} \quad (5)$$

The fitting accuracy $R^2=96/25\%$.

3 Experimental Verification

3.1 Test Survey and Measuring Point Layout

In order to verify the effectiveness of the fitted calculation model of the shock wave overpressure peak in the tunnel, the warhead explosion test in the long straight tunnel of square section with reinforced concrete was carried out on a proving ground. The tunnel used in the test is shown in Fig.6.

The size of the inner section of the tunnel is $2m \times 2m$, the thickness of both side wall and upper wall of the tunnel is 0.8m, the thickness of the bottom of the tunnel is 0.4m, the length of the tunnel is 70m, and the strength of the tunnel is C40. The charge of the warhead is 87 kg, and its equivalent TNT mass is 161 kg. During the test, the warhead was placed vertically at the geometric center of the section 5m away from one end of the tunnel, and both ends of the tunnel are open. Two shock wave pressure measuring points are set on each central axis of the plane of both sides walls and bottom wall of the tunnel respectively which are 18m, 20m, 22m, 58m, 60m and 62m away from the explosion point, so six measuring points are set at the same blast center distance in the tunnel.

The schematic of structure of shock wave pressure measurement system in the tunnel is shown in Fig.7

The pressure sensor selects the ICP piezoelectric pressure sensor produced by the American PCB company. The sensor has high acquisition accuracy and can meet the measurement requirements for blast field shock wave pressure. The data collector selects the TraNET 408S produced by ELSYS Company. Because the series of the data collector are integrated with ICP signal conditioning module, it can be directly connected to the sensor without an additional signal conditioner^[15]. And one end of the trigger signal line is tied to the warhead, and the other end is tied to the trigger controller. The



Fig.6 Physical Drawing of the Tunnel Used in the Test

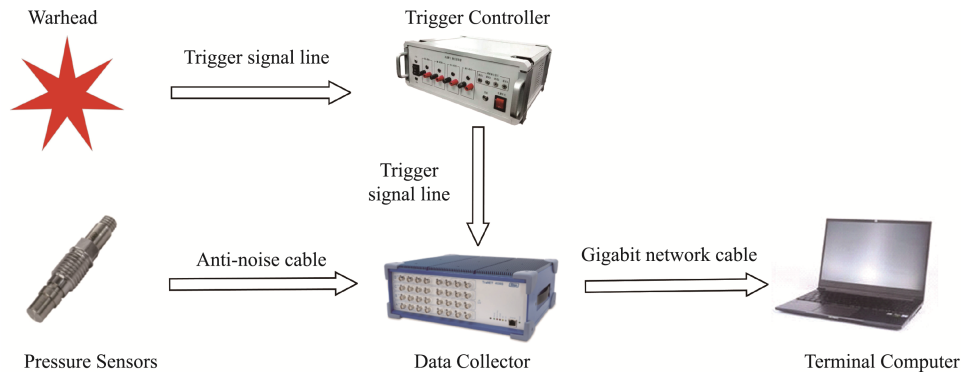


Fig.7 Schematic of Structure of Shock Wave Pressure Measurement System

trigger controller is connected to the data collector through a trigger signal line, and the pressure sensors are connected to the data collector through the anti-noise cables. The sampling frequency is set to 1MHz.

The pressure sensors are installed on the mounting panel, and the entire pressure test component is fixed to the tunnel wall using expansion screws. The anti-noise cables exposed in the tunnel are covered with angle iron and fixed with expansion screws. The two pressure sensors on the same panel of the side wall of tunnel are installed along up-down direction, the upper and lower pressure measuring points are marked A and B respectively. The two sensors of the same panel of bottom wall of tunnel are installed along the central axis, and the measuring point near the explosion center is marked A, the another point is marked B. The layout of measuring points on the test site is shown in Fig.8.

3.2 Test Result Analysis

There is a lot of natural fragment when the warhead explodes in the tunnel, the damage of the pressure sensor and anti-noise cables are more serious, the complete pressure curve measured is less, and the effective shock wave pressure curve are not measured at some measuring points. The effective shock wave pressure curves of the measuring points at the distance of 20m and 50m from the explosion center are shown in Fig.9.

It can be seen from Fig.9 that the shock wave overpressure peak of the pressure measuring points on the inner surface and bottom surface of the tunnel at the same blast center distance are almost equal in the

middle-far field. The shock wave pressure is reflected and superimposed due to the restriction of the tunnel space in the process of propagation, and the pressure curve shows multiple peaks. The shock wave pressure sustains for a long time and attenuates slowly.

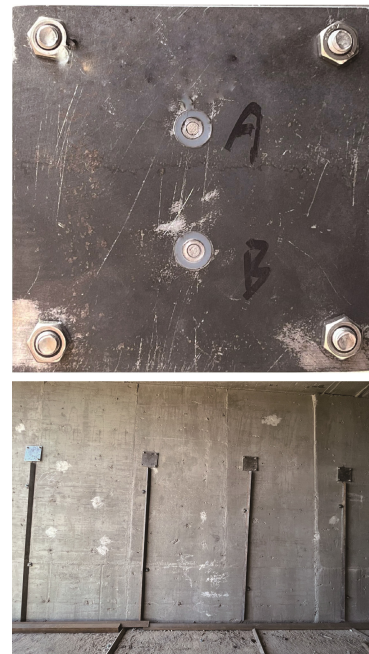


Fig.8 Measuring Point Layout at the Test Site

According to the formula (6), it is known that shock wave overpressure peak in the tunnel is mainly related to the blast center distance, the cross-sectional area of the tunnel, the mass of equivalent TNT, the strength and density of the tunnel, by substituting various physical parameters, the calculated value of the shock wave overpressure peak is obtained and compared with the actually measured value, and the results are

listed in Table 8. For convenience, the measuring points A and B of side surface 1, side surface 2 and bottom

surface at the same blast centre distance in the tunnel are numbered 1 ~ 6 in turn.

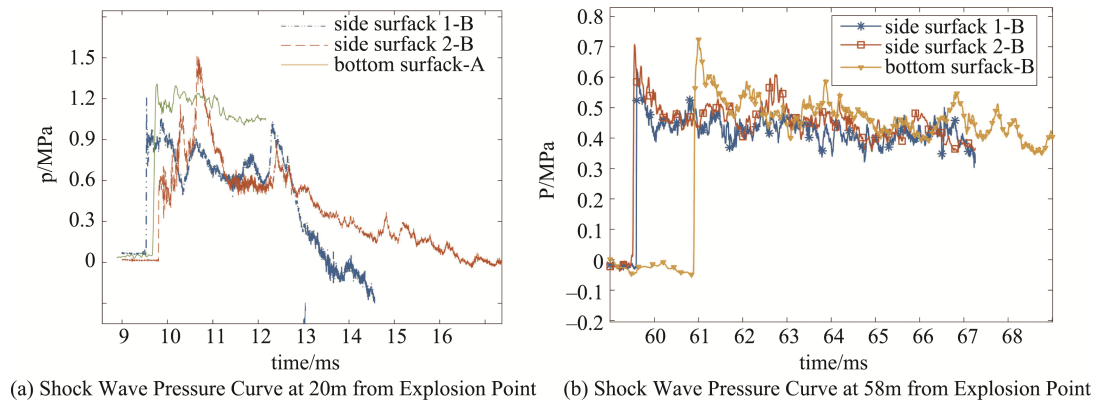


Fig.9 Actually Measured Shock Wave Pressure Curve

Table 8 Comparison Between the Measured Value and Calculated Value of Shock Wave Overpressure Peak

Blast Center Distance (m)	Measuring Point	Measured Value (MPa)	Calculated Value (MPa)	Relative Deviation
18	1	1.297	1.168	9.95%
18	2	1.302	1.168	10.30%
18	3	1.265	1.168	7.68%
18	5	1.274	1.168	8.33%
20	1	1.144	1.090	4.71%
20	4	1.220	1.090	10.68%
20	5	1.185	1.090	8.04%
22	2	0.956	1.024	7.10%
22	4	0.915	1.024	11.85%
22	5	0.941	1.024	8.77%
58	1	0.527	0.541	2.62%
58	2	0.487	0.541	11.09%
58	3	0.513	0.541	5.46%
58	4	0.531	0.541	1.89%
58	5	0.556	0.541	2.70%
60	1	0.518	0.529	2.20%
60	2	0.532	0.529	0.56%
60	5	0.499	0.529	6.01%
60	6	0.476	0.529	11.17%
62	1	0.465	0.518	11.28%
62	2	0.517	0.518	0.11%
62	3	0.526	0.518	1.58%
62	5	0.466	0.518	11.03%

4 Conclusion

(1) When the same mass of TNT explodes in tunnel with different materials, the shock wave overpressure peak and its time history curve of the measuring points

at the same blast center distance are almost equal in the near-field from the explosion center. With the increase of the blast center distance, the shock wave overpressure peak at the same measuring point is different obviously. The shock wave overpressure peak in the steel tunnel is

20.76% and 34.82% higher than those in the concrete tunnel and granite tunnel respectively, and the shock wave overpressure peak in the concrete tunnel is 24.91% higher than that in the granite tunnel.

(2) The attenuation rate of shock wave overpressure peak in tunnels with different materials showed a downward-increasing-downward trend, and the shock wave overpressure peak attenuation rates of two adjacent monitoring points in the near field range are all less than 15%. With the increase of blast center distance, the attenuation rate of shock wave overpressure peak in tunnels with different materials tends to be equal, and all remain within 5%. The shock wave pressure lasts for a long time in the tunnel and attenuates slowly.

(3) Based on dimensional analysis and combined with the results of numerical simulation, the mathematical model of shock wave pressure propagation law in the tunnel is established, and the effectiveness of the mathematical model is verified by the explosion test of the warhead in the reinforce concrete tunnel. The results show that the maximum relative deviation between the measured value and the calculated value of the shock wave overpressure peak is 11.85%. Therefore, it is proved that the mathematical model can be used to predict the shock wave overpressure peak in the tunnel with different materials, and can provide some reference for the power evaluation of warhead explosion in the tunnel.

References

- [1] Zhang Y, Wang S, Yuan J, et al. (2020). Experimental Study on the Propagation Law of Blast Waves in a Square Tunnel. *Chinese journal of energetic materials*, 28(1), pp.46-51.
- [2] Liu J B, Yan Q S, Wu J. (2009). Study on Propagation Law of Explosion Shock Wave in Tunnel. *Journal of vibration and shock*, 28(06), pp.8-11.
- [3] Ma R H, Jia B, Yang L, et al. (2022). The Influence of Tunnel Section Shape on Propagation Law. *Journal of weapon equipment engineering*, 43(02), pp.92-96.
- [4] Guo R J. (2021). Study on Propagation Law of Explosion Shock Wave in Tunnel and Dynamic Response of Tunnel. M. Eng, Nanjing University of Science and Technology.
- [5] Zhong C, Sun Y. (2022). Influence of Explosion Points Position on the Propagation Law of Shock Wave in Tunnel. Weihai, China. Springer Science and Business Media Deutschland GmbH.
- [6] Song J, Li S C, Zhang D F, et al. (2016). Study on Propagation Law of Explosion Shock Wave in Underground Space. *Journal of underground space and engineering*, 12(2), pp.560-566.
- [7] Li H, Wu H, Wang Z, et al. (2022). Experimental and Numerical Simulation of the Propagation Law of Shock Waves in Corrugated Steel-Lined Tunnels. *Process safety and environmental protection*, 168, pp.1019-1030.
- [8] Gen Z G, Li X D, Miao C Y, et al. (2017) Study on Propagation Law of Explosion Shock Wave of Thermobaric Explosive in Tunnel. *Journal of vibration and shock*, 36(05), pp.23-29.
- [9] Qu K K, Yan Y J, Liu Y, et al. (2011) Comparative Study on Propagation Law of Explosion Shock Wave in Long Straight Tunnel and Complex Tunnel. *Journal of applied mechanics*, 28(04), pp.434-438.
- [10] WANG H T, LI Z Z, SHAO L Z, et al. (2022) Numerical Simulation of Chemical Explosion Load
- [11] Value on Tunnel Blast Door. *Protective engineering*. 44(5), pp.13-20.
- [12] PAN F, GAO P F, YANG L, et al. (2013) Numerical Investigation on Blast Shock Wave Propagation of an Explosion Inside its Entrance to a Multilevel Gallery Tunnel. *Journal of safety science and technology*. 9(11), pp.48-52
- [13] LI G B, LUO Y J. (2022) ANSYS of Dynamic Response of Reinforced Concrete Beams Based on Impact Load of RHT Model. *Journal of Jilin Jianzhu university*. 39(1), pp.11-16.
- [14] Jiao X, Zhao P, Yao Y, et al. (2020) Regulation of Different Quantity TNT Blasting in Multi-Cabin Structure Based on Simulation and Dimensional Analysis. *Explosion and shock waves*. 40(8).
- [15] Wang Z, Li Y, Huang Y. (2020). Parameter Determination of JH-2 Model and Numerical Analysis of Repeated Penetration of Granite. *Journal of Harbin institute of technology*, 52(11), pp.127-136.
- [16] CHEN J H, KONG D R, XU C D, et al. (2022) Shock Wave Pressure Test and Analysis in Tunnel. *Journal of foreign electronic measurement technique*. 41(12), pp.63-68.

Author Biographies



CHEN Jiahui is currently a M.Sc. candidate in Nanjing University of Science and Technology (NJUST). His main research interest includes the explosion parameter test in constrained space.

E-mail: jh18217631591@163.com



KONG Deren received Ph.D. from Nanjing University of Science and Technology (NJUST). He is currently a professor and PhD supervisor in NJUST. His main research interest includes the test technology of dynamic parameters of weapons.

E-mail: derenkong@hotmail.com

